中国激光

基于圆偏振的高能量波长可调谐超快光纤激光研究

刘伟[1]，李中超[1]，陈润植[2]，常国庆[2*]

[1]中山大学物理与天文学院，广东 珠海 519082；

[2]中国科学院物理研究所光物理重点实验室，北京 100190

摘要 本文介绍了一种基于圆偏振光脉冲驱动的波长可调谐、能量可扩展的超快光纤光源。在光子晶体光纤中利用自相位调制占主导的非线性效应来展宽脉冲光谱，在输出端使用滤光片来选择特定的光谱旁瓣以满足后续实验需要。仿真及实验表明：在光谱展宽程度相同时，输入的圆偏振光功率需要达到线偏振光功率的1.4倍，相应的滤出光谱旁瓣能量约为线偏振光的1.4倍。进一步研究表明：圆偏振脉冲的输出光谱普遍存在比线偏振脉冲输出光谱更清晰的波瓣结构，有利于后续滤波输出过程中脉冲质量的提升；适当增加脉冲的输入功率可进一步拓宽光谱的调谐范围，在输入功率为4.9 W时，可获得波长范围为930～1200 nm的高能量飞秒脉冲。

关键词 非线性光学；圆偏振光；超快光纤激光；光子晶体光纤

中图分类号 O437 **文献标志码** A **DOI**：10.3788/CJL220605

1 引 言

超快光纤激光器具有散热性能强、单通增益高、增益带宽大、结构紧凑和装置稳定等特性，已发展成为可取代传统固态激光器的典型代表之一，在微纳加工、医疗成像、阿秒科学、自由电子激光等领域具有广阔的应用前景，并逐渐成为研究微观世界和揭示材料系统超快过程的技术手段[1-5]。在生物医学领域，为发挥多光子显微成像光学层切能力强、成像深度更大、光学损伤较小的独特优势[6-7]，科研人员对波长可调谐、能量可扩展的超快光纤激光进行了深入研究，目前，波长可调谐、能量可扩展的超快光纤激光已成为超快激光研究领域的重点内容之一。波长在800～1300 nm范围内的飞秒脉冲可以激发双光子荧光显微镜中所使用的大多数重要荧光团[8]。人们通常采用光参量振荡器[9](OPO)、超连续谱产生(SCG)[10]和基于自相位调制(SPM)的光谱旁瓣滤波等技术来拓宽超快激光的波长范围。OPO技术虽然可以产生波长范围为900～1300 nm且脉冲能量较大的宽光谱[11-12]，但OPO装置复杂、成本高昂，对于钛宝石激光而言，还需要额外的水冷装置[13]。SCG技术可将入射脉冲扩展到更短和更长的波长方向，但是SCG将输入脉冲能量分布在整个宽光谱中，在后续选择10～30 nm带宽的光谱时脉冲能量较小(<1 nJ)，光纤中的色散效应会展宽脉冲使其偏离傅里叶变换极限脉冲，即限制脉冲光谱的进一步展宽[14]。基于SPM的光谱旁瓣滤波技术——SPM-enabled spectral selection，简称为“SESS技术”，是近几年发展起来的一种产生可调谐飞秒脉冲的新技术；该技术的核心在于利用光纤中的自相位调制效应产生分立的频谱旁瓣，之后使用滤波器将中心波长最短和最长的旁瓣滤出，从而实现脉冲波长调谐。一系列理论计算和实验工作均证明了该方案不仅能够突破光纤色散、高阶孤子分裂、相位匹配等限制调谐的因素，而且具有良好的能量可扩展性，可以实现低噪声、多波长、大范围调谐的变换极限脉冲输出[15-17]。例如，研究人员基于掺镱光纤激光器系统，通过SESS技术成功获得了波长在0.825～1.21 μm之间可连续调谐的光脉冲，脉冲宽度在70～120 fs之间[8]。

众所周知，超短脉冲在光纤中传输时伴有SPM等三阶非线性效应，进而产生了丰富的非线性光纤光学现象[18]，包括光孤子、光脉冲自相似演化、SCG、脉冲自压缩等。三阶非线性效应不仅与光纤材料有关，还与入射脉冲的偏振状态有关。理论分析和实验均表明，圆偏振脉冲引起的SPM效应是线偏振脉冲的2/3。换言之，当非线性传输过程中的B积分保持不变时，采用圆偏振脉冲传输可以将脉冲能量提高约1.5倍[19]。因此，圆偏振脉冲被广泛应用于高能量光纤放大系统，包括啁啾脉冲放大系统和预啁啾管理脉冲放大系统[20-21]。

本课题组提出了使用圆偏振飞秒脉冲激发光谱旁瓣产生以提高SESS脉冲能量的方案，并通过理论分析与实验相结合的方式系统对比了圆偏振脉

收稿日期：2022-02-28；**修回日期**：2022-03-15；**录用日期**：2022-04-11；**网络首发日期**：2022-04-23

基金项目：国家自然科学基金(12175324)

通信作者：*guoqing.chang@iphy.ac.cn

冲和线偏振脉冲的非线性演化过程，实验结果与理论仿真结果非常吻合。本次研究发现，由于受激拉曼（SRS）效应与脉冲偏振无关，因此在保证光谱展宽不变的情况下，采用圆偏振脉冲能够将脉冲能量增加约 1.4 倍。

2　理论模拟

任何偏振态的超短脉冲在光纤中的非线性光谱展宽都可以用耦合广义非线性薛定谔方程（CGNLSE）精确描述[22]，即

$$\frac{\partial A_+}{\partial z}+\sum_{n\geqslant 2}\frac{\mathrm{i}^{n+1}\beta_n\partial^n A_+}{n!\ \partial T^n}=\gamma\left(\mathrm{i}-\frac{1}{\omega_0}\frac{\partial}{\partial T}\right)\left\{f_{\mathrm{R}}A_+\int_{-\infty}^{\infty}h_{\mathrm{R}}(T-t')\left[\left|A_+(t')\right|^2+\left|A_-(t')\right|^2\right]\mathrm{d}t'+(1-f_R)A_+\left[\frac{2}{3}\left|A_+\right|^2+\frac{4}{3}\left|A_-\right|^2\right]\right\},\tag{1}$$

$$\frac{\partial A_-}{\partial z}+\sum_{n\geqslant 2}\frac{\mathrm{i}^{n+1}\beta_n\partial^n A_-}{n!\ \partial T^n}=\gamma\left(\mathrm{i}-\frac{1}{\omega_0}\frac{\partial}{\partial T}\right)\left\{f_{\mathrm{R}}A_-\int_{-\infty}^{\infty}h_{\mathrm{R}}(T-t')\left[\left|A_+(t')\right|^2+\left|A_-(t')\right|^2\right]\mathrm{d}t'+(1-f_R)A_-\left[\frac{2}{3}\left|A_-\right|^2+\frac{4}{3}\left|A_+\right|^2\right]\right\},\tag{2}$$

式中：A_+和A_-分别代表脉冲右旋偏振态分量和左旋偏振态分量的缓慢包络近似振幅；$\beta_n(n=1,2,\cdots)$表示光纤中的第n阶色散系数；$\gamma=\frac{\omega_0 n_2}{c\cdot A_{\mathrm{eff}}}$表示光纤的非线性系数，其中$\omega_0$为脉冲中心角频率，$n_2$为非线性折射率系数，$c$为真空中的光速，$A_{\mathrm{eff}}$为有效模场面积；$f_{\mathrm{R}}$代表非线性效应中拉曼响应的部分贡献，$f_{\mathrm{R}}=0.18$；$h_{\mathrm{R}}(t)$为拉曼响应函数；$t'$为拉曼响应的时间延迟；$T=t-\beta_1 z$，其中$\beta_1$为一阶色散项。

为了解各偏振光脉冲在光子晶体光纤中传输的光谱展宽差异，本课题组采用上述耦合广义非线性薛定谔方程进行了初步仿真。为了与实验一致，仿真时尽可能采用实验中测量的数据。初始高斯脉冲的中心波长设置为 1030 nm，未补偿色散为 7000 fs^2，脉冲半峰全宽为 190 fs，重复频率为 55 MHz，选用长度为 7 cm 的 LMA-8 光纤。图 1 表示此脉冲在不同输入功率下的光谱演化，其中图 1(a)是线偏振脉冲在非线性光纤中的光谱演化，图 1(b)是圆偏振脉冲在非线性光纤中的光谱演化。如图 1 所示，随着输入功率从 0 增大至 4 W，线偏振脉冲的输出光谱逐渐展宽，光谱最右端已达到 1400 nm，而此时圆偏振脉冲仅达到了 1200 nm。只有当输入功率进一步提升至 5.6 W 时，圆偏振脉冲的光谱才与线偏振脉冲呈现出相同的分布。

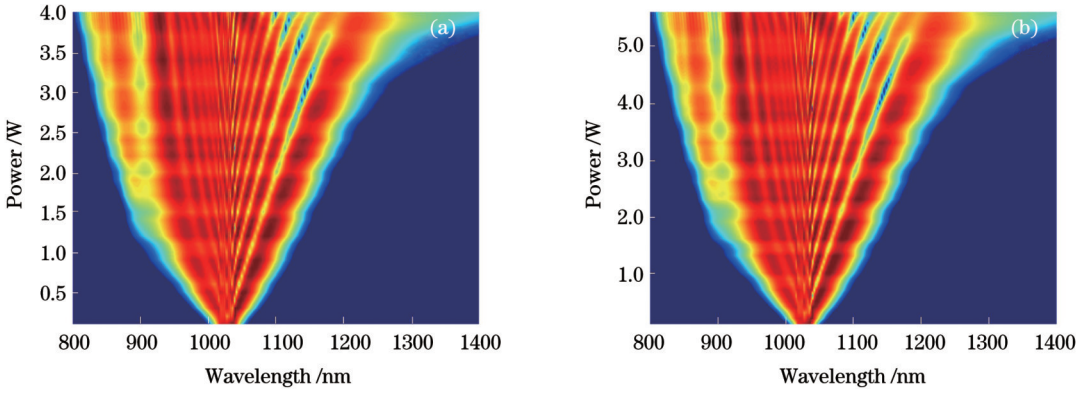

图 1　线偏振脉冲和圆偏振脉冲在非线性光纤中输出光谱的演化。(a)线偏振脉冲；(b)圆偏振脉冲

Fig. 1　Output spectra evolution of linearly and circularly polarized pulses in nonlinear optical fiber. (a) Linearly polarized pulse; (b) circularly polarized pulse

为了更清晰地进行比较，进一步绘制了图 2，以展示在相同光谱展宽量下不同偏振态（线偏振态与圆偏振态）输入脉冲的输出光谱。如图 2(a)所示，两种偏振脉冲的输出光谱几乎完全重合，区别仅在于两者的输入功率不同。为了使光谱右侧展宽到 1.2 μm，圆偏振（CP）脉冲的输入功率需要达到 4.9 W，而线偏振（LP）脉冲的输入功率仅需 3.6 W。如图 2(b)所示，为了使光谱右侧的旁瓣频移至 1.1 μm，圆偏振脉冲和线偏振脉冲的功率要求分别为 2.1 W 和 1.5 W。

可以发现：在相同的展宽量下，圆偏振脉冲所需能量约为线偏振脉冲的 1.4 倍。当用于光谱展宽的光纤色散接近零（实验中所用光纤的色散系数小，且光纤长度较短）时，在光纤中传输的脉冲的左旋和右旋偏振态分量在时域上保持不变，此时倍率可以由式(1)或式

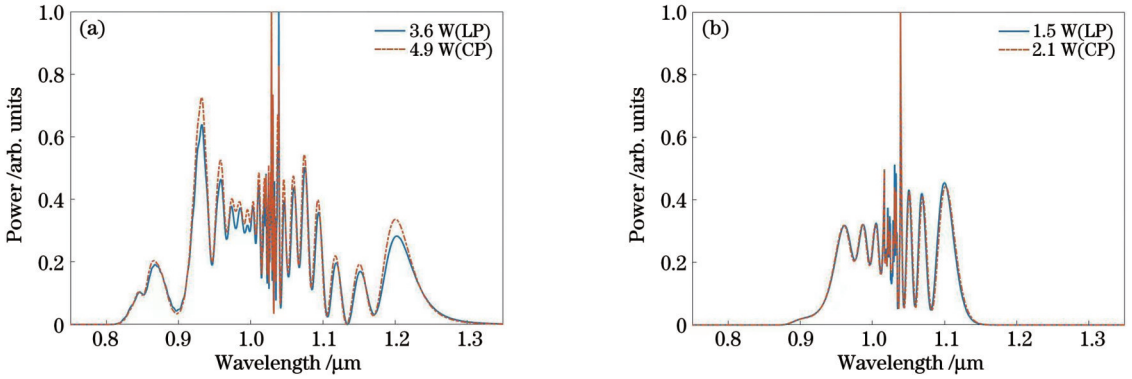

图 2 不同偏振态输入脉冲在相同光谱展宽情况下的输出光谱，其中实线代表线偏振脉冲，虚线代表圆偏振脉冲。(a)右侧旁瓣峰频移至 1.2 μm；(b) 右侧旁瓣峰频移至 1.1 μm

Fig. 2 Output spectra of input pulses with different polarization states in the same spectral broadening, where solid line represents linearly polarized (LP) pulse and dotted line represents circularly polarized (CP) pulses. (a) Peak frequency of right-side lobe is shifted to 1.2 μm; (b) peak frequency of right-side lobe is shifted to 1.1 μm

(2)简易计算得出。以式(1)为例，假设脉冲的总峰值功率为$|A|^2=|A_+|^2+|A_-|^2$，非线性强度可近似表示为$\gamma\left(f_R|A|^2+(1-f_R)\left[\frac{2}{3}|A_+|^2+\frac{4}{3}|A_-|^2\right]\right)$。当输入为线偏振态时，$|A_+|^2=|A_-|^2=\frac{1}{2}|A_L|^2$，非线性强度为$\gamma|A_L|^2$；当输入为圆偏振态时，$|A_-|^2=0$，$|A_+|^2=|A_C|^2$，非线性强度约为$0.727\gamma|A_C|^2$。当$|A_C|^2=1.38|A_L|^2$时，两者的非线性强度才会相同。这种性质表明圆偏振输入有利于光纤光源获得更高的脉冲能量。

除了线偏振脉冲和圆偏振脉冲外，椭圆偏振脉冲的光谱展宽也有其独特的性质。当线偏振光通过1/4波片时，如果线偏振光的振动面与波片光轴的夹角为45°，线偏振光就会变成圆偏振光；如果线偏振光的振动面与波片光轴的夹角不等于45°，线偏振光就会变成椭圆偏振光。将上述初始脉冲的功率调整为3.5 W，并重新模拟其圆偏振态和两种椭圆偏振态的情况，两种椭圆偏振态分别对应输入线偏振方向与1/4波片光轴夹角为47°(43°)和49°(41°)的情况。三种情况下的模拟结果如图3所示。可见，椭圆偏振脉冲和圆偏振脉冲的输出光谱在0.85～1.23 μm波段内完全相同，仅在光谱两端存在差异。椭圆偏振脉冲的光谱两侧隆起了旁瓣，这源于椭圆偏振脉冲中较弱的圆偏振分量所受到的强烈交叉相位调制的影响。假设椭圆偏振脉冲中较弱的圆偏振分量为$A_+\left(|A_+|^2<\frac{|A|^2}{2}\right)$，其非线性强度可以近似表示为$\gamma\left\{f_R|A|^2+(1-f_R)\left[\frac{2}{3}|A|^2+\frac{2}{3}|A_-|^2\right]\right\}\left(|A_-|^2>\frac{|A|^2}{2}\right)$。从公式的形式不难看出，$A_+$的强度越弱，$A_-$的强度越强，脉冲的

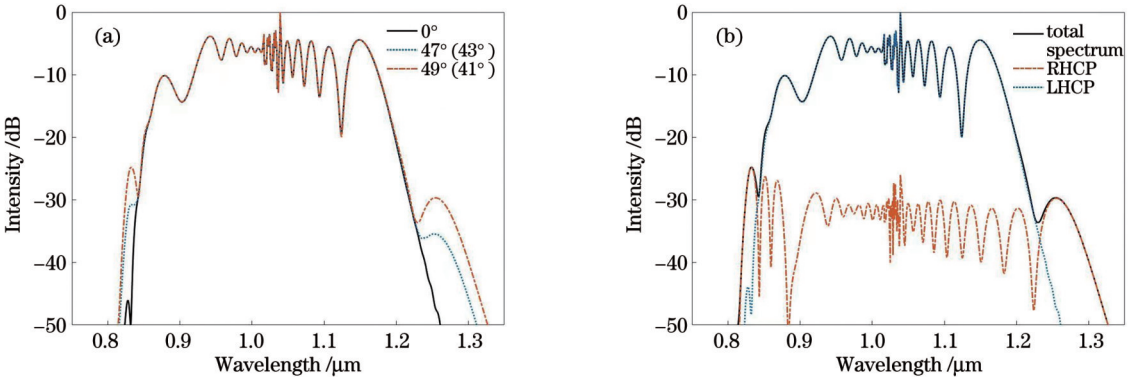

图 3 输出光谱图。(a)不同偏振脉冲的输出光谱图，实线代表线偏振光的振动面与波片光轴的夹角为45°，短虚线代表线偏振光的振动面与波片光轴的夹角为47°(43°)，长虚线代表线偏振光的振动面与波片光轴的夹角为49°(41°)；(b)右旋偏振态分量THCP和左旋偏振态分量LHCP的输出光谱图

Fig. 3 Output spectra. (a) Output spectra of pulses with different polarization states, where solid line represents the angle between vibration plane of linearly polarized light and optical axis of wave plate is 45°, short dotted line represents the angle is 47° (43°), and long dotted line represents the angle is 49° (41°); (b) output spectra of right-handed and left-handed polarization state components

椭偏程度越大，A_+分量整体的非线性强度也就越高，从而光谱展宽程度也就越大。

3　实验分析

为了验证上述模拟结果的正确性，本课题组搭建了如图4所示的实验装置。此装置由前端的光纤啁啾脉冲放大(CPA)系统和后端SESS系统两部分构成。整个CPA系统结构紧凑且性能稳定，系统主要包括光纤振荡器、一段展宽光纤、两段掺镱增益光纤和一对透射光栅。由振荡器发出种子脉冲，种子脉冲的中心波长为1030 nm，重复频率为55 MHz。种子激光经脉冲展宽、两级放大和光栅对压缩后可输出平均功率为8 W、半峰全宽为190 fs的飞秒脉冲，该飞秒脉冲作为后端SESS系统的输入。与模拟参数一致，该SESS系统同样基于一段长度为7 cm的LMA-8光子晶体光纤。该光纤的模场直径为7.5 μm，零色散波长约为1160 nm，色散系数D为−21 ps/(km·nm)。实际输入功率可通过旋转偏振光束分光器(PBS)前端的半波片进行调节；PBS后端的1/4波片用于控制输入脉冲的偏振态，使输入脉冲在线偏振态、圆偏振态和椭圆偏振态之间切换。具有某种偏振态的光脉冲耦合进入光子晶体光纤后，受多种非线性效应的影响，输出光谱会大幅展宽，而滤光片或双色镜负责滤出所需的光谱分量，实现波长可调谐输出。

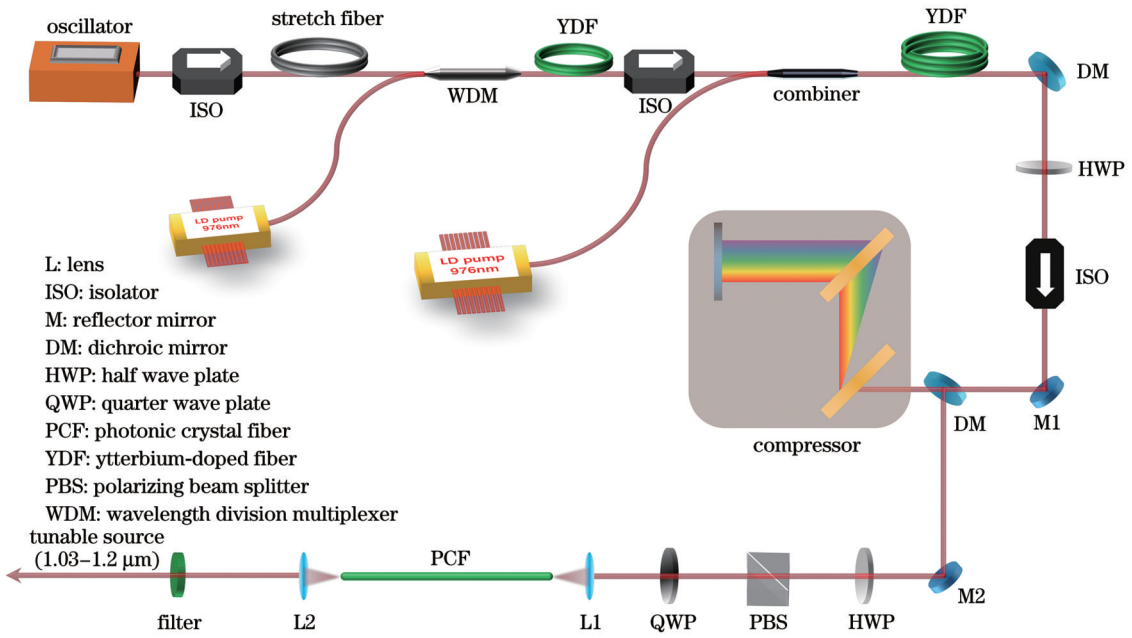

图4　高能量波长可调谐超快光纤激光系统实验装置图

Fig. 4　Experimental setup of high energy, wavelength tunable and ultrafast fiber laser system

图5显示了线偏振脉冲和圆偏振脉冲的输出光谱随输入功率变化的实验结果。与图1所示的模拟结果一致：随着输入功率增大，线偏振脉冲和圆偏振脉冲输出光谱的宽度均呈线性增加的趋势；在输入功率一致的情况下，圆偏振脉冲的光谱展宽程度明显弱于线偏振脉冲。如图5所示，当输入功率提升至3.45 W时，线偏振脉冲光谱右侧的旁瓣就已频移到1200 nm，而此时圆偏振脉冲光谱右端的旁瓣仅在1150 nm左右，

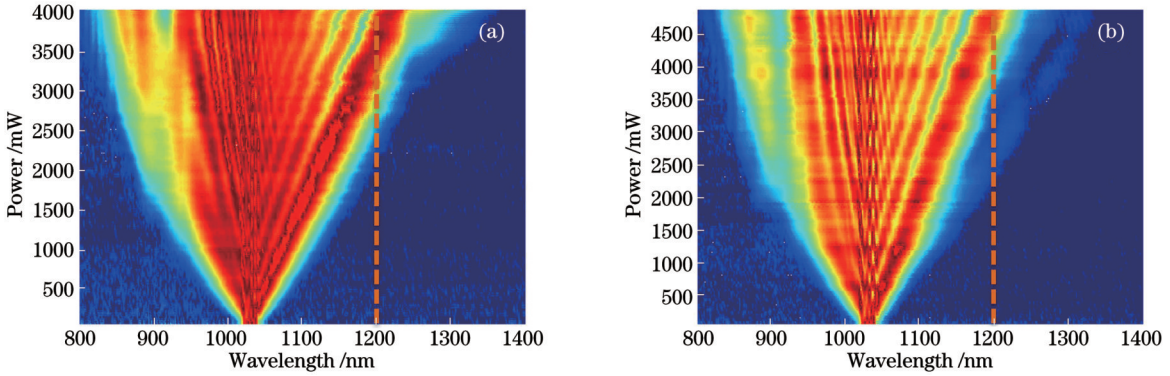

图5　不同偏振输入脉冲在不同功率下的输出光谱，其中虚线标定了1200 nm波段。(a)线偏振脉冲；(b)圆偏振脉冲

Fig. 5　Output spectra of input pulses with different polarization states at different powers, where dotted line demarcates 1200 nm band. (a) Linearly polarized pulse; (b) circularly polarized pulse

直到功率提升至4.9 W时，圆偏振脉冲的光谱才展宽至1200 nm。圆偏振脉冲与线偏振脉冲的输入功率比为1.42，很接近理论预测结果（约为1.4）。此外，可以发现，在相同的光谱展宽程度下，圆偏振脉冲的光谱结构更加清晰。

为了更加精确地验证线偏振脉冲和圆偏振脉冲在相同光谱展宽下的输入功率比，仿照图2中的模拟结果，在图6中绘制出了线偏振脉冲和圆偏振脉冲在相同光谱展宽情况下的输出光谱。图6（a）为光谱右旁瓣频移至1100 nm的情况，此时线偏振脉冲所需的输入功率为1.5 W，而圆偏振脉冲所需的输入功率为2.1 W，后者与前者之比为1.4；图6（b）、（c）分别对应光谱右旁瓣频移至1150 nm和1200 nm的情况，此时线偏振脉冲的输入功率分别为2.55 W和3.45 W，而圆偏振脉冲的输入功率则需提升至3.55 W和4.9 W，圆偏振脉冲与线偏振脉冲的输入功率比分别为1.39和1.42。这三种情况下的实验结果都十分符合上述理论模型的预测，这意味着对于相同的输出波长，采用圆偏振态输入的方法能将SESS系统的输出功率提高1.4倍左右。此外，如图6所示，与线偏振脉冲输出光谱相比，圆偏振脉冲输出光谱具有更深的沟壑和更清晰的波瓣结构，圆偏振脉冲有利于后续的滤波过程，进而提升输出脉冲的质量。

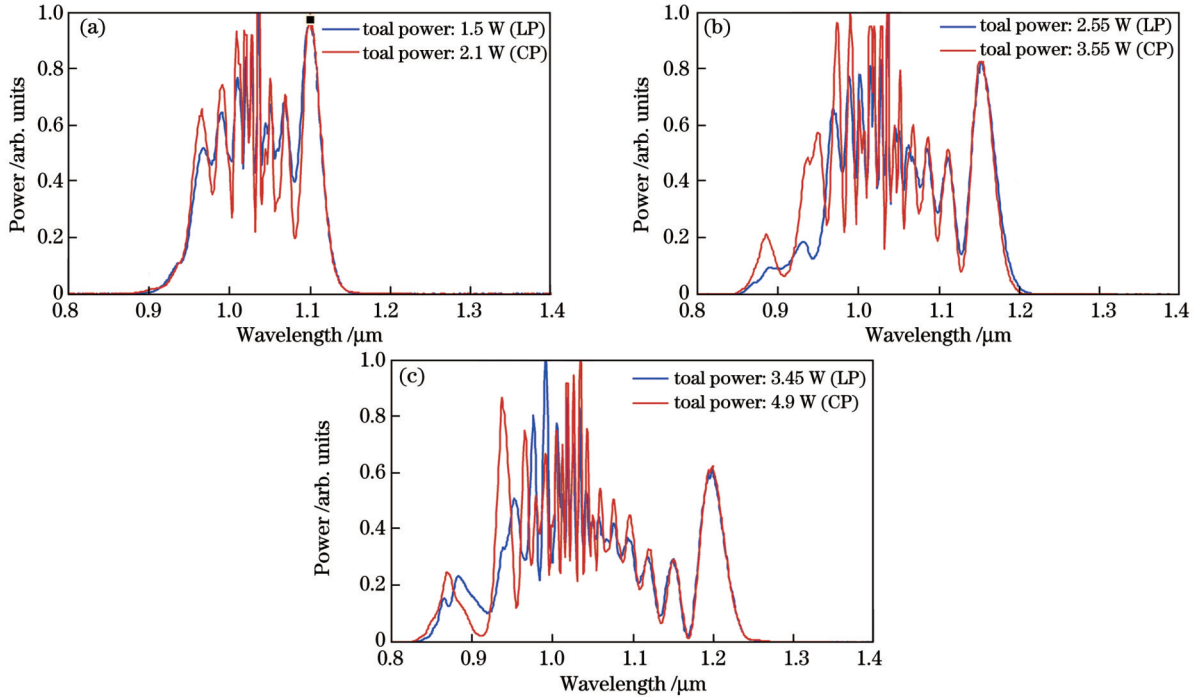

图6 不同偏振输入脉冲在相同光谱展宽情况下输出光谱的实验结果。（a）右侧旁瓣峰频移至1100 nm；（b）右侧旁瓣峰频移至1150 nm；（c）右侧旁瓣峰频移至1200 nm

Fig. 6 Experimental results of output spectra of input pulses with different polarization states under the same spectral broadening. (a) Peak frequency of right-side lobe shifts to 1100 nm; (b) peak frequency of right-side lobe shifts to 1150 nm; (c) peak frequency of right-side lobe shifts to 1200 nm

在圆偏振脉冲光谱展宽实验的基础上，本课题组又进一步通过实验验证了椭圆偏振脉冲光谱展宽的性质。与模拟所用的参数相同，输入功率调节为3.5 W。通过将1/4波片的光轴旋转至与水平偏振方向的夹角分别为45°、45°±2°和45°±4°，得到了三种不同的输出光谱，分别对应圆偏振态和两种椭圆偏振态。三种光谱的实验结果如图7所示，其中椭圆偏振脉冲和圆偏振脉冲输出光谱的强度分布在0.87～1.23 μm范围内大致相同，而在光谱两侧，椭圆偏振脉冲比圆偏振脉冲多出了明显的旁瓣。这与图3所示的模拟结果完全一致，充分印证了理论模拟的准确性。

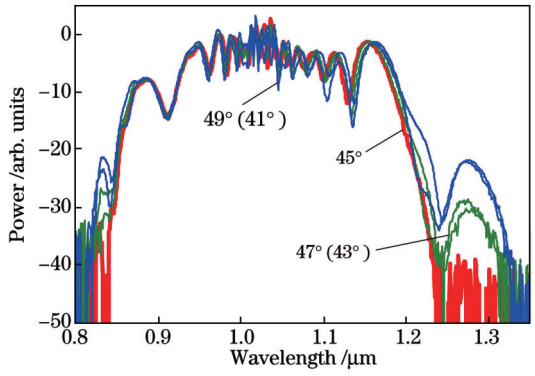

图7 圆偏振脉冲和椭圆偏振脉冲的输出光谱

Fig. 7 Output spectra of circularly polarized pulse and elliptically polarized pulses

4 结 论

本文介绍了一种基于圆偏振光的波长可调谐、能量可扩展的超快光纤光源。采用CPA技术对低功率种子光进行功率放大，输出了功率恒定且性能稳定的信号光；通过调节半波片和PBS调整耦合进入光子晶体光纤的脉冲功率，通过调节1/4波片改变入射脉冲的偏振态，利用非线性效应展宽光谱，最后通过双色镜或滤光片选择特定的光谱旁瓣。通过仿真和实验发现：在光谱展宽程度相同时，以圆偏振光入射所获得的输出功率约为线偏振光的1.4倍，而且输出光谱普遍存在比线偏振脉冲输出光谱更深的沟壑和更清晰的波瓣结构，有利于后续滤波过程中脉冲质量的提升；同时，适当增加脉冲的输入功率可以进一步拓宽光谱的调谐范围。最后，进一步对椭圆偏振脉冲进行研究发现，椭偏程度越大，交叉相位调制影响就会越强，脉冲光谱展宽就会增大。

综上所述，当入射功率达到4.9 W时，基于圆偏振脉冲激发的SESS系统能获得可在930～1200 nm波段范围内调节的高能量飞秒脉冲，非常适合用于驱动多光子显微镜实现对生物医学组织的大深度成像。

参 考 文 献

[1] Fermann M E, Hartl I. Ultrafast fibre lasers[J]. Nature Photonics, 2013, 7(11): 868-874.

[2] Chang G Q, Wei Z Y. Ultrafast fiber lasers: an expanding versatile toolbox[J]. iScience, 2020, 23(5): 101101.

[3] 刘一州, 乔文超, 高空, 等. 高功率超快光纤激光技术发展研究[J]. 中国激光, 2021, 48(12): 1201003.
Liu Y Z, Qiao W C, Gao K, et al. Development of high-power ultrafast fiber laser technology[J]. Chinese Journal of Lasers, 2021, 48(12): 1201003.

[4] Shi W, Fang Q, Zhu X S, et al. Fiber lasers and their applications [J]. Applied Optics, 2014, 53(28): 6554-6568.

[5] 董自凯, 宋晏蓉. 光纤激光器被动锁模技术研究进展[J]. 中国激光, 2021, 48(5): 0501006.
Dong Z K, Song Y R. Research progress of mode-locked fiber lasers based on saturable absorbers[J]. Chinese Journal of Lasers, 2021, 48(5): 0501006.

[6] Guo L, Wong M S. Multiphoton excited fluorescent materials for frequency upconversion emission and fluorescent probes[J]. Advanced Materials, 2014, 26(31): 5400-5428.

[7] Helmchen F, Denk W. Deep tissue two-photon microscopy[J]. Nature Methods, 2005, 2(12): 932-940.

[8] Liu W, Li C, Zhang Z G, et al. Self-phase modulation enabled, wavelength-tunable ultrafast fiber laser sources: an energy scalable approach[J]. Optics Express, 2016, 24(14): 15328-15340.

[9] 王菲菲, 聂鸿坤, 刘俊亭, 等. 小型化宽调谐MgO: PPLN中红外纳秒光参量振荡器[J]. 中国激光, 2021, 48(5): 0501015.
Wang F F, Nie H K, Liu J T, et al. Miniaturized widely tunable MgO: PPLN nanosecond optical parametric oscillator[J]. Chinese Journal of Lasers, 2021, 48(5): 0501015.

[10] 田康振, 李耀程, 任和, 等. 脊形芯硫系光纤的制备及其线偏振超连续谱的产生[J]. 激光与光电子学进展, 2021, 58(21): 2106001.
Tian K Z, Li Y C, Ren H, et al. Fabrication of chalcogenide fiber with ridged core and its linearly polarized supercontinuum spectrum generation[J]. Laser & Optoelectronics Progress, 2021, 58(21): 2106001.

[11] Ganikhanov F, Carrasco S, Xie X S, et al. Broadly tunable dual-wavelength light source for coherent anti-Stokes Raman scattering microscopy[J]. Optics Letters, 2006, 31(9): 1292-1294.

[12] Galletti M, Pires H, Hariton V, et al. Ultra-broadband near-infrared NOPAs based on the nonlinear crystals BiBO and YCOB [J]. High Power Laser Science and Engineering, 2020, 8: e29.

[13] Xu C, Wise F W. Recent advances in fibre lasers for nonlinear microscopy[J]. Nature Photonics, 2013, 7(11): 875-882.

[14] Tzeng Y W, Lin Y Y, Huang C H, et al. Broadband tunable optical parametric amplification from a single 50 MHz ultrafast fiber laser[J]. Optics Express, 2009, 17(9): 7304-7309.

[15] Zhou G J, Cao Q, Kärtner F X, et al. Energy scalable, offset-free ultrafast mid-infrared source harnessing self-phase-modulation-enabled spectral selection[J]. Optics Letters, 2018, 43(12): 2953-2956.

[16] Chung H Y, Liu W, Cao Q, et al. Megawatt peak power tunable femtosecond source based on self-phase modulation enabled spectral selection[J]. Optics Express, 2018, 26(3): 3684-3695.

[17] Chen R Z, Chang G Q. Pre-chirp managed self-phase modulation for efficient generation of wavelength-tunable energetic femtosecond pulses[J]. Journal of the Optical Society of America B, 2020, 37(8): 2388-2397.

[18] Agrawal G P. Nonlinear fiber optics: its history and recent progress [J]. Journal of the Optical Society of America B, 2011, 28(12): A1-A10.

[19] Schimpf D N, Seise E, Eidam T, et al. Advantage of circularly polarized light in nonlinear fiber-amplifiers[J]. Proceedings of SPIE, 2010, 7580: 75802E.

[20] Liu W, Schimpf D N, Eidam T, et al. Pre-chirp managed nonlinear amplification in fibers delivering 100 W, 60 fs pulses[J]. Optics Letters, 2015, 40(2): 151-154.

[21] Schimpf D N, Eidam T, Seise E, et al. Circular versus linear polarization in laser-amplifiers with Kerr-nonlinearity[J]. Optics Express, 2009, 17(21): 18774-18781.

[22] Agrawal G. Nonlinear fiber optics[M]// Nonlinear fiber optics. Amsterdam: Elsevier, 2012.

Wavelength-Tunable Ultrafast Fiber Laser with High Energy Based on Circularly Polarized State

Liu Wei[1], Li Zhongchao[1], Chen Runzhi[2], Chang Guoqing[2*]

[1]*School of Physics and Astronomy, Sun Yat-Sen University, Zhuhai* 519082, *Guangdong, China*;

[2]*Key Laboratory of Optical Physics, Institute of Physics, Chinese Academy of Sciences, Beijing* 100190, *China*

Abstract

Objective Ultrafast fiber lasers have many advantages, such as excellent heat removal, high single-pass gain, compactness.

Moreover, it has numerous applications in fundamental research and industry, particularly in the biomedicine area. The wavelength tunability of ultrafast laser is one of the most demanding features for multiphoton microscopy imaging. For instance, in two-photon fluorescence microscopy, most fluorophores can be excited by femtosecond pulses in the 800–1300 nm wavelength range. Techniques such as optical parametric oscillator (OPO), supercontinuum generation (SCG), and self-phase modulation enabled spectral selection (SESS) are commonly used to generate such kinds of lasers. Although OPO can generate ultrafast pulses with broad spectral and high pulse energy, it is quite expensive and not user-friendly. SCG can generate an octave-spanning spectrum; however, the pulse energy is far lower than 1 nJ. SESS has been developed recently to generate tunable femtosecond pulses. The core of this scheme is to generate discrete spectral side-lobes enabled by the self-phase modulation-dominated nonlinear effect. A series of theoretical calculations and experiments have shown that this scheme can overcome the wavelength tuning restrictions such as fiber dispersion, high-order soliton fission, Raman effect, etc. The $\chi^{(3)}$ nonlinear effect is generally understood to be connected not only to the fiber material but also to the polarization state of the incident pulse. When the B-integral is constant in the nonlinear transmission process, both theory and experiments suggest that circularly polarized pulse transmission can enhance the energy of pulses by approximately 1.5 times.

Methods In this study, we fabricated an ultrafast fiber laser with tunable wavelength and scalable energy using circularly polarized pulses. The system consists of the front-end driven laser (fiber CPA laser) and the following spectral broadening and selection unit (SESS). The central wavelength of a home-built ultrafast-driven laser is 1030 nm. The maximum average power is 8 W, and the repetition rate is 55 MHz. The SESS unit comprises photonic crystal fiber, launching power adjustment setup, and spectral selection filter. The half-wave plate and PBS are used to modify the input power, while a 1/4-wave plate regulates the polarization state of the input pulse. The filter or dichroic mirror is responsible for filtering out the appropriate spectral components to produce output with wavelength adjustable.

Results and Discussions The SESS and CPA systems are the major parts of the high-energy wavelength-tunable ultrafast fiber laser (Fig. 4). As the input power increases, the broadening of the output spectrum based on linearly and circularly polarized pulses displays a proportional increase. The spectral broadening of circularly polarized pulses is less than that of linearly polarized pulses when the input power is the same in two polarization states. The rightmost side-lobe of the linearly polarized pulse shifts to 1200 nm when the input power is increased to 3.45 W, and the power of the circularly polarized laser increases to 4.9 W to reach a similar spectral broadening. The power ratio of the two is 1.42, which is consistent with the results obtained via theoretical simulation. Furthermore, we discovered that the spectral structure of circularly polarized pulses is more distinct with the same degree of spectral broadening (Fig. 2 and Fig. 5). We compared their spectra to validate the input power ratio of the linear and circular polarization pulses under the same spectral broadening condition. When the spectrum's rightmost lobe is shifted to 1100 nm, the power in the linear polarization state is 1.5 W, while the power in the circularly polarized state will increase to 2.1 W, implying that the ratio is approximately 1.4. The linearly polarized pulse's input power is 2.55 W and 3.45 W, respectively, when switching to 1150 nm and 1200 nm, while the circularly polarized pulse's power is 3.55 W and 4.9 W, corresponding to power ratios of 1.39 and 1.42, respectively. The practical results of the three cases are consistent with our theoretical model, showing that using the circularly polarized pulse can boost the output power by around 1.4 times (Fig. 6). Furthermore, the output spectrum in a circularly polarized state has deeper modulation and a clearer lobe structure than the linearly polarized pulses, which benefits the subsequent filtering process and increases the stability of output pulse. Finally, a study on elliptically polarized pulses has discovered that the broadened spectrum shows broader but weak lobes due to the occurrence of cross-phase modulation exceptionally in elliptical polarization states (Fig. 3 and Fig. 7).

Conclusions This study introduces a circularly polarized ultrafast fiber laser with tunable wavelength and scalable energy. The ultrafast input pulses spectrum is strongly broadened in PCF by nonlinear effects dominated by self-phase modulation. Furthermore, we filter out the desired spectral side-lobes with an optical filter, which will be a promising method for generating the light source with high energy and exotic wavelength. The theoretical and experimental studies show that, with the same degree of spectral broadening, the input power of circularly polarized pulses is about 1.4 times higher than that of linear polarized pulses, and the corresponding filtered out energy can be increased by about 1.4 times. Simultaneously, the study shows that circularly polarized pulses tend to have a larger wavelength tuning range by increasing the input power. Finally, this study presentes a high-energy femtosecond laser with a wavelength tuning range between 930 and 1200 nm by the self-phase modulation enabled spectral broadening method. This laser can be a promising alternative for driving multiphoton microscopy to enable high penetration depth imaging of biomedical tissue.

Key words nonlinear optics; circularly polarized light; ultrafast fiber laser; photonic crystal fiber